RESEARCH ARTICLE

DNA mismatch repair activity of MutLα is regulated by CK2-dependent phosphorylation of MLH1 (S477)†

Abbreviated title: Phosphorylation of MLH1

Isabel M. Weßbecher[1], Inga Hinrichsen [1], Sebastian Funke[2], Thomas Oellerich[3], Guido Plotz[1], Stefan Zeuzem[1], Franz H. Grus[2], Ricardo M. Biondi[1,4], Angela Brieger[1]*

[1]Medical Clinic I, Biomedical Research Laboratory, Goethe-University, Frankfurt a.M., Germany
[2]Experimental Ophthalmology, Department of Ophthalmology, University Medical Center, Gutenberg University, Mainz, Germany
[3]Department of Medicine II, Hematology/Oncology, Goethe-University, Frankfurt a.M., Germany
[4]Instituto de Investigación en Biomedicina de Buenos Aires (IBioBA)-CONICET-Partner Institute of the Max Planck Society, Buenos Aires, Argentina

*Correspondence should be addressed to A.B. (a.brieger@em.uni-frankfurt.de)

***Corresponding author**: Angela Brieger, PhD
Medical Clinic I,
Biomedical Research Laboratory
Goethe-University
Theodor-Stern-Kai 7
D-60590 Frankfurt a.M.
Germany
Phone: +49 - 69 - 6301 – 6218
Fax: +49 - 69 - 6301 - 87689
Email: a.brieger@em.uni-frankfurt.de

†This article has been accepted for publication and undergone full peer review but has not been through the copyediting, typesetting, pagination and proofreading process, which may lead to differences between this version and the Version of Record. Please cite this article as doi: [10.1002/mc.22892]

Additional Supporting Information may be found in the online version of this article.

Received 4 May 2018; Revised 22 June 2018; Accepted 18 August 2018
Molecular Carcinogenesis

DOI 10.1002/mc.22892

Grant support

This work was supported by the Wilhelm Sander Foundation [2015.161.1] and the Deutsche Krebshilfe [109651] and did not receive any funding from a commercial company.

Abbreviations

MMR, DNA mismatch repair; CK2, Casein kinase II; ATM/ATR, Ataxia-telangiectasia-mutated/ataxia telangiectasia and Rad3-related; PI3K, phosphoinositide 3-kinase; TBB, 4,5,6,7-tetrabromobenzotriazole; CamKII, Calcium/Calmodulin-dependent protein kinase II; TMCB, 2-(4,5,6,7-Tetrabromo-2-(dimethylamino)-1H-benzo[d]imidazol-1-yl)acetic acid; TTP22, 3-[[5-(4-Methylphenyl)thieno[2,3-d]pyrimidin-4-yl]thio]propanoic acid; His, Hexahistidine;

Abstract

MutLα, a heterodimer consisting of MLH1 and PMS2, is a key player of DNA mismatch repair (MMR), yet little is known about its regulation. In this study, we used mass spectrometry to identify phosphorylated residues within MLH1 and PMS2. The most frequently detected phosphorylated amino acid was serine 477 of MLH1. Pharmacological treatment indicates that Casein kinase II (CK2) could be responsible for the phosphorylation of MLH1 at serine 477 *in vivo*. *In vitro* kinase assay verified MLH1 as a substrate of CK2. Most importantly, using *in vitro* MMR assay we could demonstrate that p-MLH1^{S477} lost MMR activity. Moreover, we found that levels of p-MLH1^{S477} varied during the cell cycle. In summary, we identified that phosphorylation of MLH1 by CK2 at amino acid position 477 can switch off MMR activity *in vitro*. Since CK2 is overexpressed in many tumors and is able to inactivate MMR, the new mechanism here described could have an important impact on tumors overactive in CK2.

Keywords: DNA mismatch repair; MLH1; MutLα; phosphorylation; CK2, Lynch syndrome.

Introduction

The MMR system performs the postreplicative correction of base-base mismatches and insertion-deletion loops resulting from defective DNA replication. Dependent on the mismatch the recognition in humans is performed by MutSα (consisting of MSH2 and MSH6 and mainly responsible for recognition of single base-base and small insertion deletion loops) or MutSβ (consisting of MSH2 and MSH3 and primarily responsible for the recognition of insertion-deletion loops containing up to 16 extra nucleotides in one strand) [1]. It has been shown, however, that there is a significant overlap between MutSα and MutSβ for the repair of insertion deletion mismatches, with MutSα playing a critical role in the repair of small (1-2) nucleotide insertion deletion mismatches [2]. After MMR initiation, MutLα (a human heterodimeric complex formed by MLH1 and PMS2) interacts with the MutS complex. MutLα, which harbors an endonuclease function, is likely to play an important role in both 5' and 3' directed MMR and is required for the recruitment of other proteins involved in further steps of the process [2,3].

Germline mutations of MMR genes are responsible for the generation of Lynch syndrome, a disease mainly associated with colon cancer and one of the most common adult-onset hereditary tumor syndromes described so far [4]. One-third of the detected MLH1 gene alterations causing defective proteins are non-synonymous, non-truncating variants, always missense variants, in the coding region [5,6]. In 12-17% of sporadic colon cancer patients, loss of MLH1 is induced by promoter hypermethylation. Although of great importance, the regulation of MMR proteins' functionality is only poorly understood. The Casein kinase II (CK2) has been described to be involved in the phosphorylation of MSH2 and MSH6 which resulted in an increased binding to mismatches [7]. Romeo et al. demonstrated BRCA1 dependent phosphorylation and

instability of MLH1 which is attributed to Ataxia-telangiectasia-mutated/ataxia telangiectasia and Rad3-related (ATM/ATR) activity [8] and Jia et al. postulated a role of phosphoinositide 3-kinase (PI3K)/AKT signaling pathway in phosphorylation and regulation of PMS2 stability [9]. Very recently, our group could show that phosphorylation-dependent degradation of PMS2 is mediated by its C-terminus and that treatment with the multi kinase inhibitor Sorafenib could inhibit this degradation process [10].

To get further insights into the regulation of MutLα we analyzed the phosphorylation of MLH1 and PMS2 in more detail, identified one highly promising phosphorylation site within MLH1 and determined its consequences for the function of MutLα in MMR.

Material and Methods

Cells

HEK293 cells (ATCC® CRL-1573™), SW480 cells (CCL-228) and SW620 cells (CCL-227), purchased from the American Type Culture Collection (Rockville, MD), and HEK293T cells, obtained from Dr. Kurt Ballmer (Paul Scherrer Institute, Villigen, Switzerland), were grown in DMEM with 10% FCS. As previously described, MLH1 is not expressed in HEK293T [11].

Sf9 cells (ATCC® CRL-1711™) were purchased from the American Type Culture Collection (Rockville, MD).

Antibodies, recombinant Proteins and Plasmids

Anti-MLH1 (G168-728) and anti-PMS2 (A16-4) were purchased from Pharmingen (BD Biosciences, Heidelberg, Germany), anti-beta Actin (Clone AC-15) was from Sigma-Aldrich (Munich, Germany). Anti-phospho-AKT-substrate (23C8D2), hereinafter

referred to as anti-p-MLH1 and anti-Cyclin B1 (D5C10) were obtained from Cell Signaling (New England Biolabs GmbH, Frankfurt, Germany). Anti-MLH1 (N-20), anti-PMS2 (E-19) and anti-Cyclin E (HE12) were from Santa Cruz (Santa Cruz Biotechnology, Heidelberg, Germany). Anti-fluorescence labeled goat anti-rabbit IRDye800CW and anti-fluorescence labeled goat anti-mouse IRDye680LT were from LI-COR (LI-COR Biosciences GmbH, Bad Homburg, Germany).

Recombinant human CK2 alpha 1 subunit was purchased from Proteinkinase.biz (Biaffin GmbH & Co KG, Kassel, Germany).

The pcDNA3.1+/MLH1 and pcDNA3.1+/PMS2 expression plasmids were described previously [12]. In addition, the MLH1-variants MLH1^{S477A}, MLH1^{D478A} and MLH1^{E480A} were generated by site-directed mutagenesis (for detailed primer information see supplementary table 1) and overexpressed in HEK293T cells.

All plasmids were confirmed by sequencing. All oligonucleotides were purchased from Sigma-Aldrich (Munich, Germany).

pEGFP_C1 plasmid (negative control plasmid for the MMR assay) was purchased from Clontech Laboratories.

Transient transfection and drug treatment

Transient transfection or cotransfection of HEK293T cells was carried out as described previously [13]. In brief, HEK293T were cotransfected at 50-70% confluence with the following expression plasmids as indicated: pcDNA3.1+/MLH1 wild type (wt) or pcDNA3.1+/MLH1 variants together with pcDNA3.1+/PMS2 wt using 20 µl/ml of the cationic polymer polyethylenimine (Polysciences, Warrington, PA; stock solution 1 mg/ml). 48 h post transfection cells were directly harvested or incubated for 8 h in Opti-MEM (Gibco) and treated as indicated for additional i) 16 h with Calyculin (50 nM) or 6 h with ii) CK2 inhibitor 4,5,6,7-tetrabromobenzotriazole (TBB) (75 µM), iii) AKT

inhibitor MK2206 (1 µM), iv) Calcium/Calmodulin-dependent protein kinase II (CamKII) inhibitor KN-93 (20 µM), v) CK2 inhibitor Emodin (75 µM), vi) CK2 inhibitor Silmitasertib (CX4945) (75 µM), vii) CK2 inhibitor 2-(4,5,6,7-Tetrabromo-2-(dimethylamino)-1H-benzo[d]imidazol-1-yl)acetic acid (TMCB) (75 µM), viii) CK2 inhibitor 3-[[5-(4-Methylphenyl)thieno[2,3-d]pyrimidin-4-yl]thio]propanoic acid (TTP22) (50 µM) or ix) DMSO as a control. Finally, cells were harvested and protein extracts or immunoprecipitated proteins were analyzed by Western blotting.

Western blotting

Proteins were separated on 10% polyacrylamide gels, followed by Western blotting on nitrocellulose membranes and antibody detection using standard procedures or as described previously [13].

If indicated the band intensity of the protein expression was quantified using Multi Gauge V3.2 program (Fujifilm, Tokyo, Japan).

All experiments were performed at least three times.

Phos-tag-PAGE

For mobility shift detection of MLH1 and PMS2 phosphoprotein isotypes a Phos-tag-PAGE was performed as described by Kinoshita et al. [14]. In brief, a gel consisting of a separating gel (7% w/v polyacrylamide and 357 mM Bis-tris-HCl, pH 6.8) and a stacking gel (4.0% w/v polyacrylamide and 357 mM Bis-tris-HCl, pH 6.8) was generated. The acrylamide-pendant Phos-tag ligand (Wako Pure Chemical, Osaka, Japan) (5 mM) and $Zn(NO_3)_2$ (10 mM) were added to the separating gel before polymerization. Gel electrophoresis was performed using the running buffer (pH 7.8) consisted of 50 mM Tris and 50 mM MOPS containing 0.1% w/v SDS and 5 mM sodium

bisulfite. After electrophoresis, the gel was soaked in a solution containing 25 mM Tris, 192 mM glycine, 10% v/v MeOH and 1 mM EDTA for 10 min, and then soaked in the same solution but without EDTA.

Wet Western blotting was carried out on PVDF membrane using 1xNuPAGE transfer buffer (Invitrogen, Carlsbad,CA, USA), containing 10% methanol and 0.5% sodium bisulfide (1 M). The proteins were blotted overnight in a cold room at 150 mA at least for 12 h.

Immunoprecipitation

Immunoprecipitations were carried out using 400-500 µg of whole cell extract from MutLα overexpressing HEK293T in a total volume of 500 µl precipitation buffer (50 mM HEPES-KOH (pH 7.6), 100 mM NaCl, 0.5 mM EDTA, 0.2 mM PMSF, 0.5 mM DTT, 1% Triton X-100) with 2 µg of anti-MLH1 (N-20), anti-MLH1 (G168-728) or anti-PMS2 (A16-4). After one hour of agitated incubation at 4°C, 20 µl protein G sepharose (Santa Cruz Biotechnology, Heidelberg, Germany) were added and incubation continued for 3 h. Precipitates were extensively washed in cold precipitation buffer using SigmaPrep^{TM} spin columns (Sigma, Munich, Germany). Success of washing was always confirmed by running samples without antibody in parallel. The sepharose was boiled in SDS-PAGE sample buffer for 5 min and proteins were separated on 10% polyacrylamide gels, followed by Western blotting on nitrocellulose membranes and antibody detection using standard procedures.

For immunoprecipitation of endogenous expressed MLH1 and confirming of endogenous p-MLH1^{S477} HEK293, SW480 and SW620 cells were applied by quadrupling the protocol as described above using anti-MLH1 (G168-728).

Peptide competition

Non-specific binding of the used antibody anti-p-MLH1 (anti-phospho-AKT-substrate (23C8D2)) to epitopes others than MLH1 proteins was excluded by performing an immunizing peptide blocking experiment. Before proceeding with the staining protocol, the antibody was neutralized by adding 10 µg/ml of the blocking phosphopeptide C-KRHREDpSDVEMVE (Davids Biotechnologie, Regensburg, Germany) that specifically corresponds to the p-epitope of MLH1. After overnight incubation on 4°C, which allows the blocking peptide to bind the antibody, Western blotting was carried out using standard procedures. By comparing the staining from the blocked antibody versus the antibody alone, we could show that the p-MLH1 staining was absent in the Western blot performed with the neutralized antibody and therefore specific for p-MLH1^{S477} binding.

Production and purification of recombinant MutLα

Recombinant Hexahistidine (His)-tagged MutLα, single MLH1 wt or MLH1^{S477A} variant were generated as described [15]. In brief, Baculoviruses containing pFastBac HTB-MLH1 wt, pFastBac HTB-MLH1^{S477A} or pFastBac HTB-PMS2 vectors were produced in DH10Bac^{TM} competent cells (Invitrogen, Carlsbad, CA, USA), transfected into Sf9 cells using Escort^{TM} IV Transfection Reagent (Sigma-Aldrich, Munich, Germany) and virus titer was increased by three amplifications. Exponentially growing Sf9 cells (100 ml with 2x10^6 cells/ml) were infected with 10 ml virus supernatant and, if indicated, 24 h after infection treated with Calyculin for 48 h. Whole cell extracts were harvested and incubated with 1 ml Ni-NTA agarose (Qiagen) for 1 h at 4°C. The agarose was washed ten times with 10 ml washing buffer (20 mM Hepes KOH, pH 7.6, 300 mM NaCl, 5 mM $MgCl_2$, 0.1 mM ethylene glycol bis(β-aminoethyl ether)*N*,*N*′-tetraacetic acid, 10 mM imidazole, 0.035% β-mercaptoethanol, 10% sucrose, and 0.5 mM PMSF)

and five times with washing buffer containing 100 mM NaCl. The bound protein was eluted in the same buffer without PMSF but with 250 mM imidazole. The success of protein purification was verified by Coomassie Brilliant Blue staining.

Mass spectrometry analysis

Calyculin treated phospho-enriched immunoprecipitated MutLα was analyzed by Liquid chromatography-electrospray ionization-tandem mass spectrometry (LC-ESI-MS/MS) [16] and immunoprecipitated MutLα from untreated MutLα transfected HEK293T cells, which was expected to be only weakly phosphorylated as well as purified His-tagged MutLα from Calyculin treated Sf9 cells were analyzed by Nano liquid chromatography-electrospray ionization-tandem mass spectrometry (NanoLC-ESI-MS/MS [17]. In brief, immunoprecipitated MLH1 and PMS2 samples were separated (for LC-ESI- as well as NanoLC-ESI-MS/MS) by SDS-PAGE and visualized by staining with Coomassie Brilliant Blue (exemplarily shown in supplementary figure 1). Then, distinct MLH1 and PMS2 bands were cut out of the gel. The now following protocol for LC-ESI- and NanoLC-ESI-MS/MS differs in detail:

For in-gel reduction of samples, which should be analyzed by LC-ESI-MS/MS, 100 µl of 100 mM 1:1 ammonium bicarbonate/acetonitrile (v/v) were added to each gel piece and incubated at RT for 30 min followed by adding of 500 µl of neat acetonitrile and incubation at RT until shrinking. Thereafter, the acetonitrile was removed and the gel pieces were in-gel digested with trypsin as described by Shevchenko et al. [18]. Finally, digested proteins were analyzed by LC-ESI-MS/MS as described by Funke *et al.* [16]. For samples which should be analyzed by NanoLC-ESI-MS/MS gel pieces were reduced with dithiothreitol and alkylated with iodoaceamide (both Sigma-Aldrich, Munich, Germany) and digested in-gel with trypsin (SERVA Electrophoresis GmbH, Heidelberg, Germany) in the presence of 0.1% RapiGest over night at 37°C. Phospho-

peptides were then enriched by TiO_2 chromatography (GL Sciences Inc., Tokyo, Japan) as described by Larsen *et al.* [19] followed by NanoLC-ESI-MS/MS analysis as described by Oellerich et al. [17].

Kinase assay

To determine whether CK2 can directly phosphorylate MLH1 we used recombinant His-tagged MLH1 wt as well as His-tagged MLH1^{S477A} variant generated in Sf9 cells and purchased recombinant CK2 alpha 1 (Biaffin GmbH & Co KG, Kassel, Germany). To ensure the use of completely unphosphorylated protein, 15-20 µg purified His-tagged MLH wt or His-tagged MLH1^{S477A} in a total volume of 60 µl were pre-incubated with 30 µl of Agarose-coupled-CIP (Sigma-Aldrich, Munich, Germany) for 1 h at 37°C and afterwards separated through centrifugation. Subsequently, *in vitro* kinase assay was carried out using 5 µl (1 µg) dephosphorylated MLH1 wt or MLH1^{S477A} substrate, 1.5 µl (80 units/0.6 µg) CK2 and 60 µM ATP in kinase buffer (105 mM Tris, 20 mM Mg^{2+}, 0.03% β-mercaptoethanol, 0.1 mg/ml BSA) in a total volume of 15 µl for 30 min at 37°C. Reaction was stopped by adding 2x concentrated Laemmli buffer (Sigma Aldrich, Munich, Germany) and heating for 5 min at 95°C. Finally, SDS-PAGE and Western blot analysis were performed to visualize the generation of phosphorylated MLH1 and to verify CK2 activity.

Measurement of MMR activity

The MMR activity of MLH1 variants was scored *in vitro* as described previously [20,21]. Briefly, 5 µg protein extracts of transfected HEK293T cells or 0.2 µg of recombinant His-tagged MutLα were mixed with 50 µg nuclear extract and 35 ng of DNA substrate containing an intact AseI restriction site, a G-T mismatch in between an (not digestible) EcoRV restriction site and a 3′ single-strand nick at a distance of 83 bp to guide the

MMR direction. If the tested heterodimer is fully qualified for mismatch repair, then the G-T mismatch will be corrected and the EcoRV restriction site will be restored. After incubation at 37°C (30 min), the DNA substrate was purified and digested with AseI (5 units/15 µl) and EcoRV (10 units/15 µl). The restriction fragments were separated in agarose gels, analyzed using GelDoc XR plus detection and band intensities were quantified using Image Lab version 3.0 (Bio-Rad). If the substrate is efficiently repaired the AseI and EcoRV digestion will result in three bands: a 2.0 kb band corresponding to singly AseI cut (uncorrected and in excess added) DNA substrate, a 1.2 kb and a 0.8 kb band caused by the successfully corrected and restricted EcoRV restriction site. The repair efficiency (e) was calculated as: e = (intensity of bands of repaired substrate)/(intensity of all bands of substrate). This result is independent of the amount of DNA recovered through plasmid purification. The repair efficiency (e) of MutLα variants was analyzed in direct comparison with MutLα wt that had been produced in parallel and calculated as e (relative) = e (variant)/e (wild-type) × 100.

Cell cycle synchronization

Endogenous MutLα expressing HEK293 cells were synchronized by treatment with 5 µM nocodazole (Sigma-Aldrich, Munich, Germany) to induce G2/M phase arrest. 17 h after incubation mitotic shake-off cells were obtained from gentle tapping, collected and washed twice with PBS to release cells from the nocodazole block. Thereafter, cells were resuspended in fresh media and allowed to progress with cell cycle activity. Cell harvesting was performed after 0 h, 2 h, 4 h, 8 h, 12 h and 24 h. To verify different cell cycle stages Cyclin E and Cyclin B1 expression was analyzed by Western blotting. The amount of p-MLH1^{S477} was detected after immunoprecipitation and quantified in correlation to total MLH1 levels using Multi Gauge V3.2. p-MLH1^{S477} levels were

calculated by setting the expression of total MLH1 to 100% and putting the amount of p-MLH1^{S477} in relation to it.

In parallel to cyclin expression analysis, the success of cell synchronization was verified by FACS analysis. Therefore, synchronized HEK293 cells were harvested after 0 h, 2 h, 4 h, 8 h, 12 h and 24 h, fixed with cold ethanol (70 %) for 30 min on ice and stained with 7-AAD (BD Biosciences, Heidelberg, Germany) for 10 min on ice. Cell cycle distribution was then analyzed on a LSRII/Fortessa flow cytometer (BD Biosciences, Heidelberg, Germany) using associated FACSDiva^{TM} software.

Structural analysis of MutLα

Structural evaluation has been performed using a composition of MutLα domains crystal structures and homology models whose generation has been described in detail before [22].

Statistical analysis

For comparison of the MMR assays all single values were calculated relative to the mean value of the positive control. Gaussian distribution was determined using Dallal-Wilkinson-test. P-values of MMR-Assay were estimated by using unpaired t-test or Welch's t-test for unequal variances, [23]. P-values of cell cycle dependent p-MLH1^{S477} expression levels were determined using ANOVA test. A p-value of <0.05 was considered to indicate a statistically significant difference. Statistical analyses were performed with BIAS program [24].

Results

MLH1 and PMS2 can be phosphorylated and phosphorylation has no impact on MutLα dimerization

To determine phosphorylation of the heterodimeric MutLα or its single components in detail we first enhanced the proportion of phosphorylated proteins by reducing the cellular phosphatases. Serine/threonine phosphatases were inhibited by using the selective and cell-permeable inhibitor Calyculin and tyrosine phosphatases were decreased by using the potent inhibitor Pervanadate. Subsequently, a special Phos-tag-PAGE was performed to identify the mass difference between phosphorylated and unphosphorylated MLH1 and PMS2. In the case of the presence phosphorylated amino acids in the analyzed protein the Phos-tags will bind and require an increase of protein's mass resulting in slower run on the Phos-tag-PAGE than the non-phosphorylated control. As shown in figure 1 A (lane 2) Calyculin treatment induced a clear bandshift of MLH1 as well as PMS2 which implicates that both proteins could be phosphorylated by serine/threonine kinases. In contrast, Pervanadate (figure 1 A, lane 3) failed to induce a bandshift.

Moreover, to assure that phosphorylation was responsible for the band shift we reversed the Calyculin induced process by subsequent treatment of protein extracts with Alkaline Phosphatase Calf Intestinal (CIP). CIP treatment restored the original protein size (figure 1 A, lane 4).

MLH1 and PMS2 from Calyculin treated in comparison to untreated HEK293T cells showed a band shift also on SDS-PAGE (figure 1 A, lane 6).

To exclude a phosphorylation-dependent effect on the dimerization of MutLα, co-immunoprecipitation using anti-PMS2 antibody was performed with protein extracts of Calyculin or DMSO treated MutLα overexpressing HEK293T cells. The detected

p-MLH1, MLH1 and PMS2 levels validated that the phosphorylation state has no impact on the dimerization of MLH1 with PMS2 or the stability of the MutLα complex (figure 1 B).

Mass Spec analysis detected phosphorylation of MLH1 at position S477

To specify phosphorylation sites of MutLα we first used immunoprecipitated MutLα from Calyculin treated HEK293T cells and performed LC-ESI-MS/MS. Second, immunoprecipitated MutLα from untreated HEK293T cells and purified His-tagged MutLα from Calyculin treated Sf9 cells were analyzed using the more sensitive NanoLC-ESI-MS/MS analysis. With both methods and in all cell systems the phospho-peptide HREDS*DVEMVEDDSR of MLH1 which harbors the phosphorylation at position S477 (figure 2 A-C) was detected in 100% of all identified phospho-peptides using LC-ESI-MS/MS and 61% of all detected phospho-peptides using NanoLC-ESI-MS/MS (supplementary table 2).

In addition, several other phospho-peptides were found in MLH1 using NanoLC-ESI-MS/MS and PMS2 using LC-ESI-MS/MS and NanoLC-ESI-MS/MS to a much lower extent (supplementary table 2).

Looking at the amino acid motif HREDSDVEMVEDDSR in MLH1 of other mammals, we found that this region is conserved which highlights the importance (figure 2 D).

Phosphorylated MLH1^{S477} could be specifically detected and motif modifications reduce phosphorylation of MLH1 at position S477

The detection of p-MLH1^{S477} was performed by Western blotting after immunoprecipitation of MLH1 from MutLα overexpressing HEK293T cells but also from endogenous MutLα expressing HEK293, SW480 as well as SW620 cells by using a specific antibody which recognizes the phospho-S477-motif RHREDS* of MLH1 (figure

3 A). p-MLH1^{S477} was clearly detectable in all cell lines and disappeared after CIP treatment which, however, also induced a general reduction of MLH1 (figure 3 A). The specificity of p-MLH1^{S477} detection could be additionally confirmed by peptide competition (supplementary figure 2).

As mentioned above the amino acid sequence surrounding site S477 of MLH1 is conserved in many mammalians (figure 2 D). A following stretch of acidic amino acids is often recognized by the corresponding kinase and extremely important for its enzymatic activity. To analyze whether the mutation of amino acid S477 or mutations of following acidic amino acids could avoid or significantly inhibit the phosphorylation at position S477, we generated three different MLH1 variants, MLH1^{S477A}, MLH1^{D478A} and MLH1^{E480A}, overexpressed these constructs in HEK293T cells, immunoprecipitated them and determined the presence of p-MLH1^{S477}. As shown in figure 3 B mutation of amino acids S477 resulted in loss of phosphorylation, MLH1^{E480A} showed significantly less phosphorylation than the wildtype protein and the faint band of MLH1^{D478A} was between the MLH1^{S477A} and MLH1^{E480A} phosphorylation levels.

CK2 is responsible for the phosphorylation of MLH1 at position S477

In silico analysis of MLH1 using several kinase predictors (prosite.expasy.org, phosida.com, phosphosite.org, phosphogrid.org) pointed out that serine 477 of MLH1 is theoretically phosphorylatable by CK2, AKT as well as CamKII. To identify the actually responsible kinase we treated MutLα overexpressing HEK293T cells with the CK2 inhibitor TBB, the AKT inhibitor MK2206, the CamKII inhibitor KN-93 or DMSO (negative control) and determined the presence of p-MLH1^{S477} after immunoprecipitation with anti-MLH1 (figure 4 A) or anti-PMS2 (figure 4 B). While TBB was able to block the phosphorylation of MLH1 at position S477, MK2206 or KN-93 had no or only little effect. The usage of four additional CK2 inhibitors, Emodin,

CX4945, TMCB and TPP22, which all lead to a significant reduction of p-MLH1^{S477} could confirm the involvement of CK2 in the phosphorylation of MLH1 at position S477 (figure 4 C).

Moreover, SDS-PAGE analysis of the kinase assay demonstrated that CK2 can directly phosphorylate MLH1 *in vitro* while it failed to phosphorylate MLH1^{S477A} mutant (figure 4 D).

Phosphorylation of MLH1 at position S477 blocks MMR

The influence of phosphorylation of MutLα on its MMR functionality was determined by using an *in vitro* MMR assay. Repair activity of MutLα from untreated MutLα overexpressing HEK293T cells served as positive control and was set to 100%, protein extracts from pEGFP_C1 transfected HEK293T cells were used as negative control.

First, recombinant MutLα purified from untreated as well as Calyculin treated Sf9 cells was used and the MMR function of the unphosphorylated recombinant MutLα was compared to the hyper phosphorylated version of recombinant MutLα. As shown in figure 5 A, we found that untreated recombinant MutLα was fully active and showed repair activity like the positive control while Calyculin treated hyper phosphorylated recombinant MutLα was unable to repair. MMR results using recombinant MutLα from two different approaches are exemplarily shown (figure 5 A).

Second, the relevance of phosphorylation of MLH1 at position S477 was determined by using protein extracts of MutLα overexpressing HEK293T cells and by comparing the MMR function of untreated and Calyculin treated MutLα wt or the MutLα variant consisting of MLH1^{S477A} and PMS2 wt. Western blotting of used protein extracts verified equal amounts of protein in the different cell extracts (figure 5 B, upper panel). Calyculin treatment of MutLα wt led to severe restriction of MMR (mean 49% repair activity) but failed to prevent MMR if the MLH1^{S477A} variant was used (mean 83% repair

activity). Furthermore, removal of phosphorylation by cotreatment with CIP in parallel to Calyculin clearly increased MMR function of MutLα wt (mean 70% repair activity) (figure 5 B, middle and lower panel).

P-values which were calculated in relation to untreated MutLα wt verified that MMR activity of Calyculin treated MutLα was significantly decreased (p=0.001832). In contrast, the MMR activity of Calyculin treated MLH1^{S477A} variant compared to Calyculin treated MutLα wt was significantly increased (p = 0.019343) (figure 5 B, lower panel).

Non-specific MMR independent repair was detectable and is responsible for around 30% of activity in the negative control (figure 5 A+B).

All experiments were performed at least five times.

Levels of p-MLH1^{S477} vary within the cell cycle

The MMR activity of MLH1 is of great importance for post-replication repair. Since we found that phosphorylation inhibits the MMR efficiency of MLH1, one might imagine that MLH1 is regulated by phosphorylation during the cell cycle. Therefore, differences of p-MLH1^{S477} levels should be visible during the cell cycle.

To determine the amount of p-MLH1^{S477} during the cell cycle, the endogenous level of p-MLH1^{S477} was analyzed at different time points in HEK293 cells after synchronization.

Cyclin B1 and Cyclin E expression levels served as cell cycle control and were used to associate the analyzed time points (0 h, 2 h, 4 h, 8 h, 12 h, 24 h) according to cell cycle stages (G2, G2/M, G1, S) (figure 6 A). As shown in figure 6 B the p-MLH1^{S477} levels compared to total MLH1 levels changed during the cell cycle. The amount of phosphorylated MLH1^{S477} (mean ±SD) was low during G2 phase 30(14) and reached

its maximum within M phase 58(40); 50(23). After reduction over G1 36(20) the p-MLH1^{S477} level increased again in S phase to 50(20); 51(45).

P-values which were calculated by ANOVA test, however, didn't show significant differences of p-MLH1^{S477} expression levels.

Potential role of S477 for the protein structure and function of MLH1

The protein structure of MLH1 and PMS2 is shown in figure 7. Both proteins contain N-terminal (NTD) and C-terminal (CTD) domains for which structures have been resolved. CTD and NTD are connected by a flexible, proline-rich linker region comprising approximately 200 residues. Constitutive dimerization is transmitted by the CTDs, while the NTDs have been shown to only transiently dimerize during the MutLα ATPase cycle (while ATP is bound) [25]. This transient dimerization, as well as an accompanying condensation between NTDs and CTDs, are intramolecular movements (depicted by the orange double head-arrows) which are enabled by the presence of the flexible linker region, in which serine 477 is located (figure 7).

Discussion

MLH1 plays a crucial role in MMR but has been also shown to participate in many other important cellular pathways. In the current study we identified that MLH1 can be posttranslationally phosphorylated at multiple sites but most dominantly at position S477. This finding is confirmed by phosphoproteomics screening data ([26], supplementary table 1).

To assure that the used recombinant proteins are correctly modified, protein expression was almost exclusively performed in human cells. The phosphorylation

status of recombinant purified proteins from Sf9 insect cells, which were additionally utilized in one assay, was verified by mass spectrometry.

Our present investigation demonstrated that the phosphorylation of MLH1 at position S477 is managed by CK2, an important kinase which is widely described to be involved in many different regulatory cell processes by playing a global role in the control of cell growth proliferation, cell death but also in DNA damage response and repair pathways [27]. In the latter case, it has been shown that CK2 is present in several nuclear protein complexes and has a role in chromatin remodeling and structure, transcription, or RNA metabolism [28], phosphorylates a number of proteins which are central in MMR, nucleotide excision repair, homologous and non-homologous end joining [27,29], localizes to double strand breaks [30] and was described to be relevant for the regulation of MMR initiation complex MutSα [7]. Thus, the identification of CK2 to be involved in the modification of the MMR protein MLH1 fits well with published data.

The amino acid sequences surrounding CK2 phosphorylation sites are similar in most CK2 substrates [31] and the identified phosphorylated peptide HREDS*DVEMVEDDSR harboring serine 477 of MLH1 is located exactly in between such kind of CK2 substrate motif which is S*/T*DXE. Normally, CK2 phosphorylates serine or threonine residues followed by a stretch of acidic amino acids [31,32]. Our observation that substitutions of the acidic amino acids at position D478 and E480 significantly reduce or avoid the amount of phosphorylation at serine 477 is consistent with the functional dependency of CK2 on acidic residues. A simply effect that the amino acid exchange abrogates antibody recognition can be excluded since the used anti-p-MLH1 is generated against the epitope RXRXXS*/T which is in front of the substituted amino acids and the antibody is described to be independent of the surrounding amino acid sequence [33].

Analyzing the influence of phosphorylation on the functionality of MutLα one has to keep in mind that cellular Calyculin treatment induces the accumulation of phosphorylation in the whole proteome which might possibly interfere the reaction. Phosphorylation of e.g. MutSα has been described to affect mismatch-binding activity [7] and to regulate its stability and protein level [34] and Calyculin treatment has very previously been shown by us to promote loss of PMS2 [10]. Therefore, we first isolated highly phosphorylated recombinant MutLα from Calyculin treated Sf9 cells and tested its MMR function (in parallel to purified MutLα from untreated Sf9 cells) in an assay where we added nuclear extract from untreated MutLα deficient HEK293T cells. Thus, we could show that phosphorylation of MutLα alone switches off the MMR activity. The principle of phosphorylation inhibiting protein function has been described for many other proteins before [35] and the previously published phosphoproteomics data (which include phospho-motif KRHREDSDVEMVE of MLH1) suggest that detected phosphorylation inactivates appropriate proteins in mitotic cells [26]. Our further *in vitro* data (generated using a small amount of protein extract from Calyculin treated MutLα overexpressing HEK293T cells and nuclear extract from untreated MutLα deficient HEK293T cells) showed that Calyculin treated MutLα in comparison to untreated MutLα repaired mismatches only approximately half (49%; p=0.001832) efficient which is clearly below the defined limit that comprehensive analyses have established [36,37]. The minimum repair efficiency to be considered as real MMR activity has been 70% [36] or 75% [37]. This minimum of repair efficiency in turn could be generated by using MLH1^{S477A} variant where serine 477 is substituted to alanine which avoids phosphorylation (leading to 83% repair efficiency). In addition, cotreatment of MutLα with Calyculin and CIP removes existing phosphorylation and clearly increases MMR function of MutLα (70% repair efficiency). Therefore, p-MLH1^{S477} must be considered deleterious for the MMR activity of MutLα.

Although a cell cycle dependent regulation of the activity of the MMR proteins would be assumed, several investigators reported relatively constant MMR proteins levels throughout the cell cycle [38-40] which indicates that protein levels are not of relevance. One might rather assume a posttranslational regulation of these proteins. In line with this, we could demonstrate that the amount of p-MLH1^{S477} varied (even if only to a small extent) during different cell cycle stages whereas the total amount of MLH1 was less influenced. Therefore, phosphorylation could be indeed a regulatory element of the MMR system.

The question is, how does phosphorylation of MLH1 switch off the MMR function of MutLα? Which are the consequences of phosphorylation? We hypothesize that phosphorylation at position S477 might inhibit the ability of MLH1 to interact with MMR process essential proteins. Although S477 is localized very close to the beginning of the MLH1-PMS2 interacting region [41,42] our data did not show any influence on PMS2 stability. PMS2 (coexpressed with MLH1) was well expressed despite Calyculin treatment indicating that dimerization of MutLα which is essential for PMS2 stabilization [43] is not impaired. In addition, we found that CIP treated non-phosphorylated samples contain less MLH1 suggesting that phosphorylation stabilizes, rather than destabilizes, MLH1. Therefore, phosphorylation of S477 seems not to disturb MLH1 and PMS2 interaction. However, the region between amino acid 410 and 650 e.g. has been described to be relevant for interaction of MLH1 with exonuclease I [44] and exonuclease I interaction might be inhibited by phosphorylation and cause the observed loss of MMR.

It is also conceivable, that phosphorylation of MLH1 led to allosteric conformational changes which inhibit the endonuclease activity of MutLα. Allosteric conformational changes are considered to be an essential intramolecular signaling event that confers regulation of the C-terminal endonucleolytic activity by the N-terminal ATPase and

serves to transmit communications with the mismatch recognition factor MutS and a DNA clamp [45]. Inhibition of endonuclease function by phosphorylation has been previously described for yeast Holliday junction resolvase Yen1 [46].

In summary, our results demonstrate, for the first time, that the MMR function of MLH1 can be actively regulated by phosphorylation. Since dysregulation of CK2 has been reported in a number of disease states including autoimmune and inflammatory diseases and neurodegenerative disorders [47], a range of tumor types [48,49], but also in diabetes [50] and since overexpression of CK2 has been demonstrated in colorectal cancer [51] we believe that the regulation of MutLα by phosphorylation of MLH1 is an important mechanism in tumor progression.

Accessibility of original data

The mass spectrometry proteomics raw data have been deposited to the ProteomeXchange Consortium via the PRIDE [52] partner repository with the dataset identifier PXD009026 and PXD009524.

Acknowledgements

We would like to thank Sandra Passmann, Evelyn Suess, Tobias Burkard and Tabea Osthues for their technical assistance, Dr. Dimitra Bon for her help with the statistical analysis, Dr. Björn Häupl for his help to evaluate the NanoLC-ESI-MS/MS data and Dr. Andreas Weigert for his support with the FACS analysis.

The results shown in this manuscript are essentially data of the PhD thesis of Isabel Madeleine Weßbecher.

The authors declare no competing financial interests.

Author contributions

Angela Brieger conceived the presented idea. Angela Brieger, Isabel Madeleine Weßbecher and Inga Hinrichsen designed the study. Isabel Madeleine Weßbecher and Inga Hinrichsen carried out the experiments. Sebastian Funke and Thomas Oellerich performed the mass spectrometry analyses. Guido Plotz, Stefan Zeuzem, Franz H. Grus and Ricardo Miguel Biondi helped supervise the project. Angela Brieger wrote the manuscript with support from Isabel Madeleine Weßbecher, Ricardo Miguel Biondi and Inga Hinrichsen.

References

1. McCulloch SD, Gu L, Li GM. Nick-dependent and -independent processing of large DNA loops in human cells. J Biol Chem 2003;278(50):50803-50809.
2. Kunkel TA, Erie DA. DNA mismatch repair. Annu Rev Biochem 2005;74:681-710.
3. Modrich P. Mechanisms and biological effects of mismatch repair. Annu Rev Genet 1991;25:229-253.
4. Sijmons RH, Hofstra RM. Review: Clinical aspects of hereditary DNA Mismatch repair gene mutations. DNA Repair (Amst) 2015.
5. Peltomaki P, Vasen H. Mutations associated with HNPCC predisposition -- Update of ICG-HNPCC/INSiGHT mutation database. Dis Markers 2004;20(4-5):269-276.
6. Thompson BA, Spurdle AB, Plazzer JP et al. Application of a 5-tiered scheme for standardized classification of 2,360 unique mismatch repair gene variants in the InSiGHT locus-specific database. Nat Genet 2014;46(2):107-115.
7. Christmann M, Tomicic MT, Kaina B. Phosphorylation of mismatch repair proteins MSH2 and MSH6 affecting MutSalpha mismatch-binding activity. Nucleic Acids Res 2002;30(9):1959-1966.
8. Romeo F, Falbo L, Di Sanzo M et al. BRCA1 is required for hMLH1 stabilization following doxorubicin-induced DNA damage. Int J Biochem Cell Biol 2011;43(12):1754-1763.
9. Jia J, Zhang Y, Cai J et al. A novel function of protein kinase B as an inducer of the mismatch repair gene hPMS2 degradation. Cell Signal 2013;25(6):1498-1504.

10. Hinrichsen I, Wessbecher IM, Huhn M et al. Phosphorylation-dependent signaling controls degradation of DNA mismatch repair protein PMS2. Mol Carcinog 2017.
11. Trojan J, Zeuzem S, Randolph A et al. Functional analysis of hMLH1 variants and HNPCC-related mutations using a human expression system. Gastroenterology 2002;122(1):211-219.
12. Brieger A, Plotz G, Raedle J et al. Characterization of the nuclear import of human MutLalpha. Mol Carcinog 2005;43(1):51-58.
13. Brieger A, Plotz G, Zeuzem S, Trojan J. Thymosin beta 4 expression and nuclear transport are regulated by hMLH1. Biochem Biophys Res Commun 2007;364(4):731-736.
14. Kinoshita E, Kinoshita-Kikuta E. Improved Phos-tag SDS-PAGE under neutral pH conditions for advanced protein phosphorylation profiling. Proteomics 2011;11(2):319-323.
15. Kosinski J, Plotz G, Guarne A, Bujnicki JM, Friedhoff P. The PMS2 subunit of human MutLalpha contains a metal ion binding domain of the iron-dependent repressor protein family. J Mol Biol 2008;382(3):610-627.
16. Funke S, Perumal N, Beck S et al. Glaucoma related Proteomic Alterations in Human Retina Samples. Sci Rep 2016;6:29759.
17. Oellerich T, Gronborg M, Neumann K, Hsiao HH, Urlaub H, Wienands J. SLP-65 phosphorylation dynamics reveals a functional basis for signal integration by receptor-proximal adaptor proteins. Mol Cell Proteomics 2009;8(7):1738-1750.
18. Shevchenko A, Tomas H, Havlis J, Olsen JV, Mann M. In-gel digestion for mass spectrometric characterization of proteins and proteomes. Nature Protocols 2006;1(6):2856-2860.

19. Larsen MR, Thingholm TE, Jensen ON, Roepstorff P, Jorgensen TJ. Highly selective enrichment of phosphorylated peptides from peptide mixtures using titanium dioxide microcolumns. Mol Cell Proteomics 2005;4(7):873-886.

20. Plotz G, Welsch C, Giron-Monzon L et al. Mutations in the MutSalpha interaction interface of MLH1 can abolish DNA mismatch repair. Nucleic Acids Res 2006;34(22):6574-6586.

21. Hinrichsen I, Brieger A, Trojan J, Zeuzem S, Nilbert M, Plotz G. Expression defect size among unclassified MLH1 variants determines pathogenicity in Lynch syndrome diagnosis. Clin Cancer Res 2013.

22. Hinrichsen I, Schafer D, Langer D et al. Functional testing strategy for coding genetic variants of unclear significance in MLH1 in Lynch syndrome diagnosis. Carcinogenesis 2015;36(2):202-211.

23. Sachs L. Angewandte Statistik: Springer-Verlag HD NY; 2003.

24. Ackermann H. Bias - a Program Package for Biometrical Analysis of Samples. Computational Statistics & Data Analysis 1991;11(2):223-224.

25. Ban C, Junop M, Yang W. Transformation of MutL by ATP binding and hydrolysis: a switch in DNA mismatch repair. Cell 1999;97(1):85-97.

26. Olsen JV, Vermeulen M, Santamaria A et al. Quantitative phosphoproteomics reveals widespread full phosphorylation site occupancy during mitosis. Sci Signal 2010;3(104):ra3.

27. Montenarh M. Protein kinase CK2 in DNA damage and repair. Translational Cancer Research 2016;5(1):49-63.

28. Krogan NJ, Kim M, Ahn SH et al. RNA polymerase II elongation factors of Saccharomyces cerevisiae: a targeted proteomics approach. Mol Cell Biol 2002;22(20):6979-6992.

29. Montenarh M. Cellular regulators of protein kinase CK2. Cell Tissue Res 2010;342(2):139-146.

30. Olsen BB, Wang SY, Svenstrup TH, Chen BP, Guerra B. Protein kinase CK2 localizes to sites of DNA double-strand break regulating the cellular response to DNA damage. BMC Mol Biol 2012;13:7.

31. Meggio F, Pinna LA. One-thousand-and-one substrates of protein kinase CK2? FASEB J 2003;17(3):349-368.

32. Allende JE, Allende CC. Protein kinases. 4. Protein kinase CK2: an enzyme with multiple substrates and a puzzling regulation. FASEB J 1995;9(5):313-323.

33. Zhang F, Lu YJ, Malley R. Multiple antigen-presenting system (MAPS) to induce comprehensive B- and T-cell immunity. Proc Natl Acad Sci U S A 2013;110(33):13564-13569.

34. Hernandez-Pigeon H, Quillet-Mary A, Louat T et al. hMutS alpha is protected from ubiquitin-proteasome-dependent degradation by atypical protein kinase C zeta phosphorylation. J Mol Biol 2005;348(1):63-74.

35. Liu YF, Herschkovitz A, Boura-Halfon S et al. Serine phosphorylation proximal to its phosphotyrosine binding domain inhibits insulin receptor substrate 1 function and promotes insulin resistance. Mol Cell Biol 2004;24(21):9668-9681.

36. Raevaara TE, Korhonen MK, Lohi H et al. Functional significance and clinical phenotype of nontruncating mismatch repair variants of MLH1. Gastroenterology 2005;129(2):537-549.

37. Takahashi M, Shimodaira H, Andreutti-Zaugg C, Iggo R, Kolodner RD, Ishioka C. Functional analysis of human MLH1 variants using yeast and in vitro mismatch repair assays. Cancer Res 2007;67(10):4595-4604.

38. Meyers M, Theodosiou M, Acharya S et al. Cell cycle regulation of the human DNA mismatch repair genes hMSH2, hMLH1, and hPMS2. Cancer Res 1997;57(2):206-208.

39. Klingler H, Hemmerle C, Bannwart F, Haider R, Cattaruzza MS, Marra G. Expression of the hMSH6 mismatch-repair protein in colon cancer and HeLa cells. Swiss Med Wkly 2002;132(5-6):57-63.

40. Meyers M, Wagner MW, Hwang HS, Kinsella TJ, Boothman DA. Role of the hMLH1 DNA mismatch repair protein in fluoropyrimidine-mediated cell death and cell cycle responses. Cancer Res 2001;61(13):5193-5201.

41. Kondo E, Horii A, Fukushige S. The interacting domains of three MutL heterodimers in man: hMLH1 interacts with 36 homologous amino acid residues within hMLH3, hPMS1 and hPMS2. Nucleic Acids Res 2001;29(8):1695-1702.

42. Guerrette S, Acharya S, Fishel R. The interaction of the human MutL homologues in hereditary nonpolyposis colon cancer. J Biol Chem 1999;274(10):6336-6341.

43. Brieger A, Trojan J, Raedle J, Plotz G, Zeuzem S. Transient mismatch repair gene transfection for functional analysis of genetic hMLH1 and hMSH2 variants. Gut 2002;51(5):677-684.

44. Schmutte C, Sadoff MM, Shim KS, Acharya S, Fishel R. The interaction of DNA mismatch repair proteins with human exonuclease I. J Biol Chem 2001;276(35):33011-33018.

45. Pillon MC, Babu VM, Randall JR et al. The sliding clamp tethers the endonuclease domain of MutL to DNA. Nucleic Acids Res 2015;43(22):10746-10759.

46. Matos J, Blanco MG, Maslen S, Skehel JM, West SC. Regulatory control of the resolution of DNA recombination intermediates during meiosis and mitosis. Cell 2011;147(1):158-172.

47. Guerra B, Issinger OG. Protein kinase CK2 in human diseases. Curr Med Chem 2008;15(19):1870-1886.

48. O-charoenrat P, Rusch V, Talbot SG et al. Casein kinase II alpha subunit and C1-inhibitor are independent predictors of outcome in patients with squamous cell carcinoma of the lung. Clin Cancer Res 2004;10(17):5792-5803.

49. Kren BT, Unger GM, Abedin MJ et al. Preclinical evaluation of cyclin dependent kinase 11 and casein kinase 2 survival kinases as RNA interference targets for triple negative breast cancer therapy. Breast Cancer Res 2015;17:19.

50. Maeda R, Raz I, Zurlo F, Sommercorn J. Activation of skeletal muscle casein kinase II by insulin is not diminished in subjects with insulin resistance. J Clin Invest 1991;87(3):1017-1022.

51. Zou J, Luo H, Zeng Q, Dong Z, Wu D, Liu L. Protein kinase CK2alpha is overexpressed in colorectal cancer and modulates cell proliferation and invasion via regulating EMT-related genes. J Transl Med 2011;9:97.

52. Vizcaino JA, Csordas A, Del-Toro N et al. 2016 update of the PRIDE database and its related tools. Nucleic Acids Res 2016;44(22):11033.

Figure Legends

Figure 1

Phosphorylation of MutLα and its impact on dimerization

MLH1 and PMS2 were cotransfected and immunoprecipitation from Calyculin, Pervanadate or Calyculin and CIP treated HEK293T cells was performed and proteins were separated on a Phos-tag-PAGE. A clear band shift of MLH1 and PMS2 was visible after Calyulin (lane 2) but not after Pervanadate (lane 3) treatment suggesting serine/threonine phosphorylation. Cotreatment of Calyculin and CIP (lane 4) prevented the bandshift (A).

An upshift smear after Calyculin treatment of both proteins could be also detected on SDS-PAGE (lane 6) (A).

The impact of phosphorylation on dimerization and stability of MutLα was determined by performing co-immunoprecipitation of MutLα transfected HEK293T cells with anti-PMS2 antibody. The increase of p-MLH1 validated the effect of Calyculin treatment and the detection of constant MLH1 and PMS2 levels confirmed that phosphorylation has no impact on the dimerization of MLH1 with PMS2 or the stability of MutLα complex (B).

Figure 2

Phospho-peptide identification

Immunoprecipitated MLH1 was analyzed by mass spectrometry (MS). Around 80% of the detected phospho-peptides harbored phosphorylation at amino acid position S477. Amino acid S477 of MLH1 is located close to the beginning of the PSM2 interaction domain (A). The MS spectrum of MLH1 shows a promising phospho-peptide peak of

m/z 949,87 (zoom view of the monoisotopic peak *m/z* 949,87) (B). MS/MS spectrum of the *m/z* 949,87 precursor peptide leading to the identification of MLH1 peptide HREDS*DVEMVEDDSR (C). S477 surrounding amino acids of MLH1 are conserved in many mammalians which are exemplarily shown (D).

Figure 3

Phosphorylation of MLH1 at position S477 is detectable by Western blotting and depends on surrounding amino acids

Using immunoprecipitated MutLα and a specific antibody which recognizes the phospho-S477-motif of MLH1 the expression of p-MLH1^{S477} was determined in MutLα overexpressing HEK293T and in endogenous MutLα expressing HEK293, SW480 and SW620 cells with or without CIP treatment (A). p-MLH1^{S477} was well detectable in all cell lines and disappeared after CIP treatment in HEK293 and HEK293T cells.

The importance of surrounding amino acids of S477 was analyzed by comparing the amount of p-MLH1^{S477} after overexpressing MLH1 wt, MLH1^{S477A}, MLH1^{D478A} and MLH1^{E480A} in HEK293T cells (B). While p-MLH1^{S477} was well detectable in MLH1 wt overexpressing cells, MLH1^{S477A} could not be phosphorylated and MLH1^{D478A} as well as MLH1^{E480A} showed clearly reduced p-MLH1 levels.

Figure 4

CK2 is responsible for the phosphorylation of MLH1 at position S477

In silico predicted kinases, CK2, AKT and CamKII were analyzed for their involvement of MLH1 phosphorylation at position S477. Using three different kinase inhibitors TBB, MK2206 and KN-93 immunoprecipitation of MutLα transfected, inhibitor treated HEK293T cells was performed by anti-MLH1 antibody (A) or anti-PMS2 antibody (B) and p-MLH1 expression was determined.

The inhibitory effect of TBB was validated by comparing five different CK2 inhibitors TBB, Emodin, CX4945, TMCB and TTP22 (C).

In vitro kinase assay was performed by using recombinant CK2 alpha and recombinant MLH1 or MLH1^{S477A} as a substrate. The generation of p-MLH1^{S477} was monitored by Western blotting (D).

Figure 5

Phosphorylation of MutLα inhibits its MMR activity

The influence of phosphorylation of MutLα on its MMR activity was assessed by an *in vitro* MMR assay as detailed in Materials and Methods. MMR activity of protein extracts from MutLα transfected HEK293T cells served as positive control, the activity of pEGFP_C1 transfected HEK293T cell extracts was used as negative control (A+B; two left lanes). First, MMR activity of untreated recombinant MutLα and Calyculin treated recombinant MutLα, purified after expression in Sf9 cells, were compared (A). Second, MMR activity of HEK293T protein extracts from Calyculin treated MutLα, from Calyculin treated MLH1^{S477A}/PMS2 variant as well as from Calyculin and CIP cotreated MutLα transfected HEK293Tcells were analyzed (B).

Numerical values of at least five independent measurements of variants and treatments were quantified (mean ±S.D.) using Multi Gauge V3.2 program (B): untreated MutLα (positive control), 100(0); negative control (NC), 30(13); Calyculin treated MutLα, 49(17); Calyculin treated MLH1^{S477A}/PMS2, 83(16); Calyculin and CIP cotreated MutLα, 70(20). P-values were calculated by unpaired t-test or Welch's t-test. *** p=0.000004; ** p=0.001832; * p=0.019343, n.s. = not significant

Figure 6

Amount of phosphorylated MLH1^{S477} change during the cell cycle

To investigate cell cycle dependent phosphorylation of MLH1^{S477} endogenous MutLα expressing HEK293 cells were synchronized by nocodazole. The success of synchronization was verified by determining the expression of Cyclin B1 and Cyclin E at different time points after nocodazole release (0 h, 2 h, 4 h, 8 h, 12 h and 24 h), controlled by beta Actin detection (A, upper panel).

Cyclin B1 and Cyclin E levels at the different time points were compared to known cell cycle dependent cyclin expression and used to specify the cell cycle stages (A, lower panel).

Immunoprecipitation was performed using the synchronized HEK293 cells followed by MLH1 and p-MLH1 detection (B, upper panel). The p-MLH1^{S477} levels varied during different cell cycle stages, whereby the highest amount of p-MLH1^{S477} was detectable during mitosis 58(40); 50(23). Moderate p-MLH1^{S477} expression could be detected in S phase 50(20); 51(45) and a reduction of MLH1 phosphorylation was observed in G1 phase 36(20) and early G2 phase 30(14) (B, lower panel).

Expression levels of three independent experiments were quantified (mean ±S.D.) using Multi Gauge V3.2 program and normalized in relation to the highest value (A) or to total MLH1 levels (B).

The cell cycle profiles obtained by flow cytometry verified the different stages of synchronized HEK293 cells after nocodazole release (C).

Figure 7

Potential structural of p-MLH1^{S477} / PMS2 heterodimer

The biologically active structural form of MLH1 (blue) in its heterodimeric form with PMS2 (green) is shown. Serine 477 of MLH1 is located in the flexible linker region and is indicated as light blue ball (shown on the left side).

NTD: N-terminal domain; CTD: C-terminal domain; orange double head-arrows: intramolecular movements.

Supplementary Table 1

List of primers used in this study for site directed mutagenesis

Supplementary Figure 1

Coomassie blue staining of immunoprecipitates

LC-ESI - and NanoLC-ESI mass spectrometry were carried out using immunoprecipitated MutLα. The success of purification was analyzed first by Coomassie Brilliant Blue staining of SDS-gels (exemplarily shown here) followed by cutting and separation of corresponding bands for mass spectrometry.

Supplementary Table 2

Identified phosphorylation sites of MLH1 and PMS2 by mass spectrometry

Supplementary Figure 2

Peptide competition avoids p-MLH1^{S477} detection

A peptide competition was performed to verify the specificity of p-MLH1^{S477} detection by the used phospho-antibody which in principle could detect several different epitopes

harboring the amino acid sequence RXRXXS*/T*. Phosphopeptide C-KRHREDpSDVEMVE, which is exactly fitting with the corresponding MLH1 sequence was able to block the antibody binding.

Figure 1

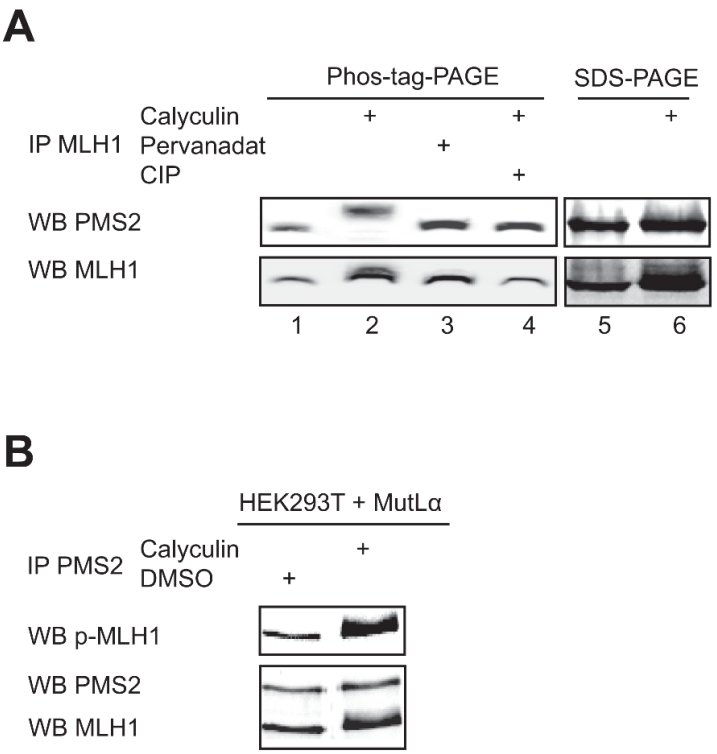

Figure 2

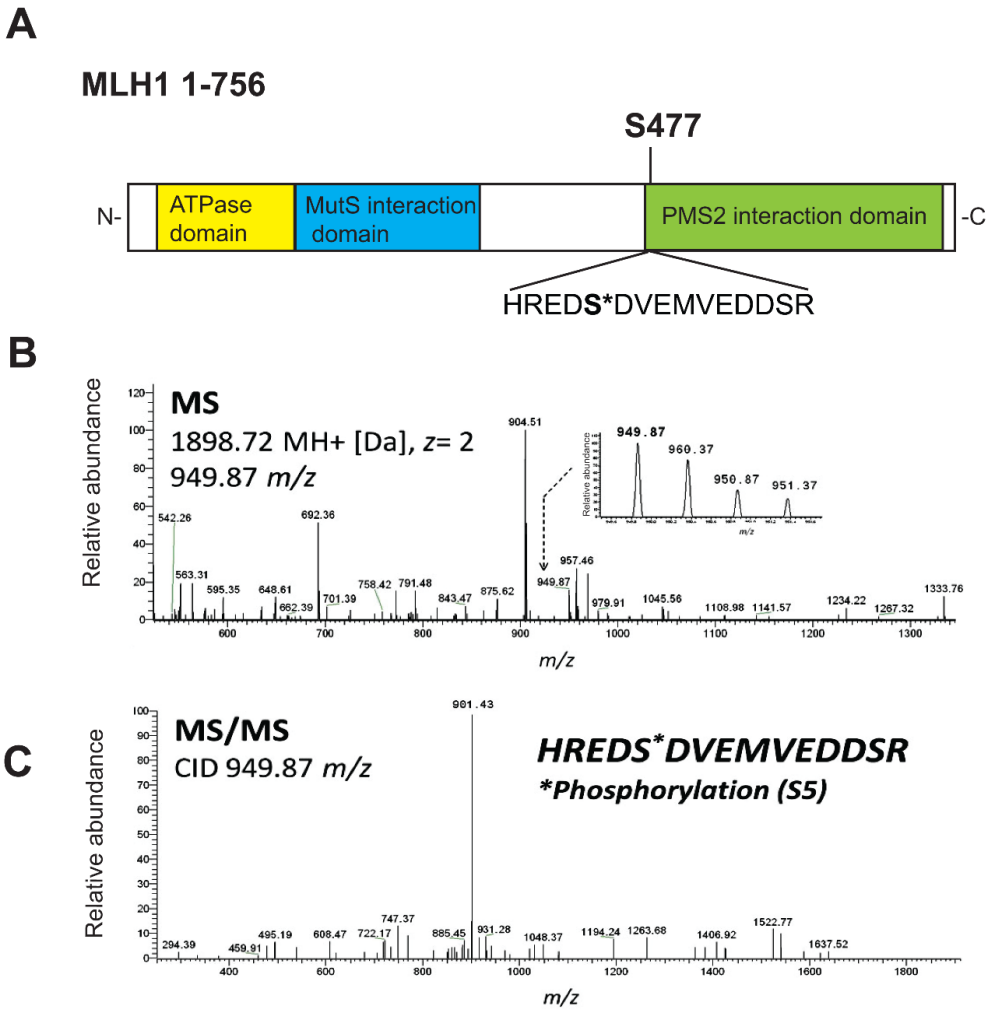

D Conserved phospho-MLH1 motif

Homo *sapiens*	HRED**S**DVEMVEDDSR
Mus *musculus*	HRED**S**DVEMVENASG
Rattus *norvegicus*	HPED**S**DVEMMENDSR
Xenopus *leavis*	PRRV**S**DVEMLEDVGS
Mesocricetus *auratus*	HRED**S**DVEMMENESR
Pan *troglodytes*	HRED**S**DVEMVEDDSR
Bos *taurus*	PRED**S**DVEMVEDASR

Figure 3

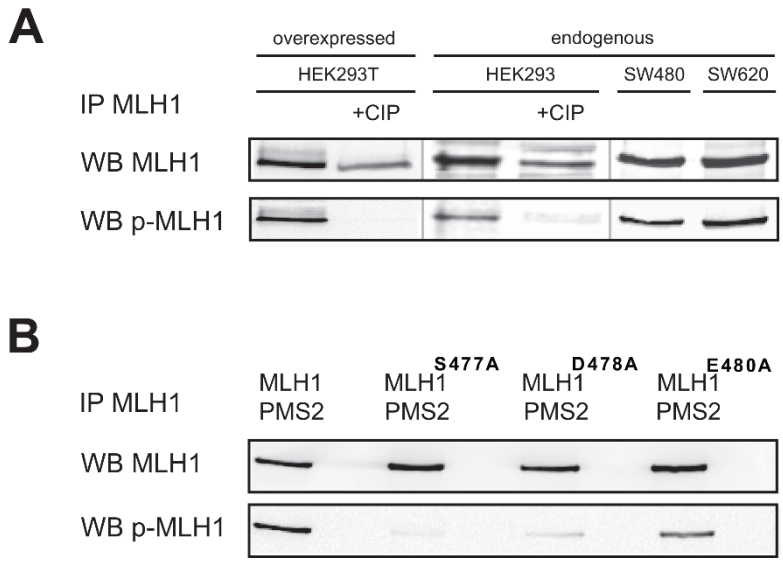

Figure 4

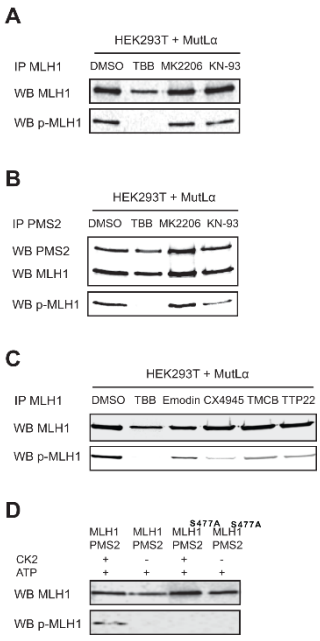

Figure 5

A

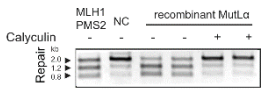

B

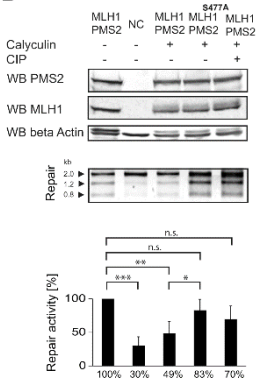

Figure 6

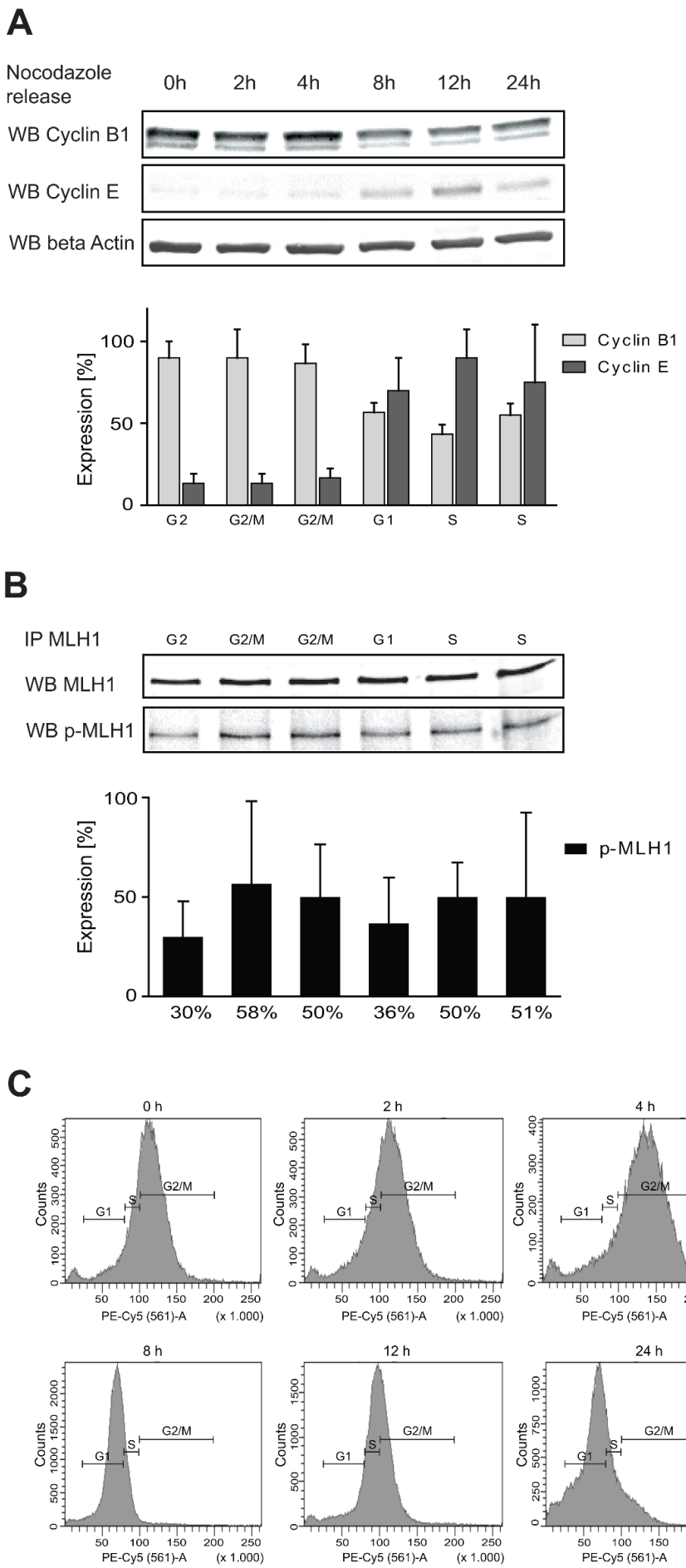

Figure 7